Neural Computing and Applications
https://doi.org/10.1007/s00521-024-09575-4

ORIGINAL ARTICLE

Deep graph-level clustering using pseudo-label-guided mutual information maximization network

Jinyu Cai[1,3] · Yi Han[2,3] · Wenzhong Guo[1] · Jicong Fan[2,3]

Received: 17 August 2023 / Accepted: 15 January 2024

Abstract
In this work, we study the problem of partitioning a set of graphs into different groups such that the graphs in the same group are similar while the graphs in different groups are dissimilar. This problem was rarely studied previously, although there has been a lot of work on node clustering and graph classification. The problem is challenging because it is difficult to measure the similarity or distance between graphs. One feasible approach is using graph kernels to compute a similarity matrix for the graphs and then performing spectral clustering, but the effectiveness of existing graph kernels in measuring the similarity between graphs is very limited. To solve the problem, we propose a novel method called Deep Graph-Level Clustering (DGLC). DGLC utilizes a graph isomorphism network to learn graph-level representations by maximizing the mutual information between the representations of entire graphs and sub-structures, under the regularization of a clustering module that ensures discriminative representations via pseudo-labels. DGLC achieves graph-level representation learning and graph-level clustering in an end-to-end manner. The experimental results on six benchmark datasets of graphs show that our DGLC has state-of-the-art performance in comparison to many baselines.

Keywords Graph neural network · Graph-level clustering · Graph kernel

1 Introduction

Graph-structured data widely exist in real-world scenarios, such as social networks [1] and molecular analysis [2]. Compared to other data formats, graph data explicitly contain connections between data through the attributes of nodes and edges, which can provide rich structural information for many applications. In recent years, machine learning on graph-structured data has gained more and more attention. Many supervised and unsupervised learning methods have been proposed for graph-structured data in various applications [3–6]. The machine learning problems of graph-structured data can be organized into two categories: node-level learning and graph-level learning. In node-level learning, the samples are the nodes in a single graph. Node-level learning mainly includes node classification [7–10] and node clustering [11–17]. Classical node classification methods are often based on graph embedding [18–20] and graph regularization [21, 22], while recent advances are based on graph neural networks (GNNs) [23–25]. Owing to the success of GNNs in node classification, a few researchers have proposed GNN-based methods for node clustering [26–29].

Different from node-level learning, in graph-level learning, the samples are a set of graphs that can be organized into different groups. Classical methods for graph-level classification are often based on graph kernels [30, 31] while recent advances are based on GNNs [32–35]. Researchers generally utilize various types of GNN, e.g.,

✉ Wenzhong Guo
guowenzhong@fzu.edu.cn

✉ Jicong Fan
fanjicong@cuhk.edu.cn

Jinyu Cai
jinyucai1995@gmail.com

Yi Han
119020013@link.cuhk.edu.cn

1 College of Computer and Data Science, Fuzhou University, Fuzhou 350116, Fujian, China

2 School of Data Science, The Chinese University of Hong Kong, Shenzhen 518172, Guangdong, China

3 Shenzhen Research Institute of Big Data, Shenzhen 518172, Guangdong, China

graph convolutional network (GCN) [23] and graph isomorphism network (GIN) [24] to learn graph-level representations by aggregating inherent node information and structural neighbor information in graphs; then, they train a classifier based on the learned graph-level representations [36–39]. Nevertheless, collecting large amounts of labels for graph-level classification is costly in real problems, and the clustering on graph-level data is much more difficult than that on nodes and still remains an open issue. It thereby shows the importance of exploring graph-level clustering, namely partitioning a set of graphs into different groups such that the graphs in the same group are similar while the graphs in different groups are dissimilar.

Previous research on graph-level clustering is very limited. The major reason is that it is difficult to represent graphs as feature vectors or quantify the similarity between graphs in an unsupervised manner [40]. An intuitive approach to graph-level clustering is to perform spectral clustering [41–44] over the similarity matrix that is produced by graph kernels [45–47] based on subgraph, random walk, etc. Although there have been a few graph kernels such as random walk kernel [48] and Weisfeiler-Lehman kernel [49], most of them rely on manual designs that may not provide desirable generalization capability for various types of graphs and produce satisfactory similarity matrices for spectral clustering, which will be demonstrated in Sect. 4.3.

Another solution comes with the encouraging development of GNNs. Some latest works such as GCN [5, 23] and GIN [24] have been proven to be effective in learning node/graph-level representations for various downstream tasks, e.g., node clustering [27, 50, 51] and graph classification [37, 52, 53] thanks to the powerful generalization and representation learning capability of deep neural networks. Therefore, it may be possible to achieve graph-level clustering by performing classical clustering algorithms such as k-means [54] and spectral clustering over the graph-level representations produced by various unsupervised graph representation learning methods [37, 55, 56].

Although the aforementioned GNN-based unsupervised graph-level representation learning methods have shown promising performance in terms of some downstream tasks such as node clustering and graph classification, they do not guarantee to generate effective features for the clustering tasks on entire graphs. In contrast, graph-level clustering may benefit from an end-to-end framework that can learn clustering-oriented features in graph-level representation learning. We summarize our motivation here: (1) Graph-level clustering is an important problem but it is rarely studied, though there have been a lot of works on graph-level classification and node-level clustering. (2) The performance of graph kernels followed by spectral clustering and two-stage methods (deep graph-level feature learning followed by k-means or spectral clustering) have not been well explored. (3) An end-to-end deep learning-based graph-level clustering method is expected to outperform graph kernels and the two-stage methods because the feature learning is clustering-oriented. Therefore, we propose a novel graph clustering method called deep graph-level clustering (DGLC) in this paper. The proposed method is a fully unsupervised framework and yields clustering-oriented graph-level representations via jointly optimizing two objectives: representation learning and clustering. The main contributions of this paper are summarized as follows:

- We investigate the effectiveness of various graph kernels as well as unsupervised graph representation learning methods in the problem of graph-level clustering.
- We propose an end-to-end graph-level clustering method. In the method, the clustering objective can guide the representation learning for entire graphs, which is demonstrated to be much more effective than those two-stage models in this paper.
- We conduct extensive comparative experiments of graph-level clustering on six benchmark datasets. Our method is compared with five graph kernel methods and four cutting-edge GNN representation learning methods, under the evaluation of three quantitative metrics and one qualitative (visualization) metric. Our method has state-of-the-art performance.

2 Preliminaries

The notations used in this paper are shown in Table 1. In the next two subsections, we briefly introduce graph kernels and GNN-based graph-level representation learning methods. We will also illustrate how to apply them to graph-level clustering.

2.1 Graph kernels

Graph kernels are typically used in both supervised and unsupervised learning that exploit graph topology. They aim to learn graph representation implicitly with predetermined graph sub-structures. For a graph G, after its subgraphs $\{G_i\}$ are defined, the kernel is calculated according to the occurrences of the sub-graphs of $\{G_i\}$. Namely, $\mathcal{K}_g(G_m, G_n) := \mathcal{F}_{G_m}^{\top}\mathcal{F}_{G_n}$, where $\mathcal{F}_{G_i}$ denotes frequency. In recent years, much effort has been devoted to the identification of desirable sub-graphs ranging from Graphlet kernel [57], Random walk kernel [30], Shortest-path kernel [58] to Subgraph matching kernel [59], Pyramid match

Table 1 Notations for the main variables and parameters in this paper

$\mathcal{G}$	Graph set	$\bar{G}$	Graph set in a minibatch
G	A single graph	V	Node set
E	Edge set	$\mathcal{X}$	Node features set
$\mathcal{N}(v)$	Neighborhood set of node v	K	Number of GNN hidden layers
$\mathbf{h}_v^k$	Learned feature for node v in k-th GNN layer	$\mathbf{a}_v^k$	Aggregated feature for node v in k-th GNN layer
$\mathbf{H}_\phi(G)$	Graph-level representation	$I_{\phi,\psi}$	Mutual information estimator
f_θ	Cluster projector	$\mathbf{Z}_{\phi,\theta}(G)$	Cluster embedding
c	Number of clusters	ϕ	Parameters of GNN
ψ	Parameters of mutual information estimator	θ	Parameter of clustering network

kernel [60], etc. For example, one of the most popular kernels is the Weisfeiler-Lehman kernel [49]. It belongs to the subtree kernel family and could scale up to large and labeled graphs. Weisfeiler-Lehman kernel is built upon other base kernels through Weisfeiler-Lehman test of isomorphism on graphs. The essential idea of the Weisfeiler-Lehman kernel is to relabel the graph with not only the original label of each vertex, but also the sorted set of labels of its neighbors (subtree structure). With a runtime scaling only linearly in the number of edges of the graphs, the Weisfeiler-Lehman kernel is widely applied in computational biology and social network analysis. However, the Weisfeiler-Lehman kernel's hashing step is somewhat ad-hoc, with performance varying from data to data [45]. Another state-of-the-art algorithm is the shortest-path kernel [58], which is based on paths instead of conventional walks and cycles. By transforming the original graph into shortest-paths graph $\tilde{G}_{v,u,e} = \{$the number of occurrences of vertex v and u connected by shortest-path $e\}$, it avoids the high computational complexity of graph kernels based on walks, subtrees, and cycles. In this paper, several graph kernels are selected as comparative models to test their efficiency in clustering. More specifically, we perform spectral clustering with the similarity matrices computed by graph kernels. One limitation is that existing graph kernels are not effective enough to quantify the similarity between graphs. In addition, most of them cannot take advantage of the node's features and labels of graphs. The related results and time complexity comparison can be found in Tables 3, 4 and 5 and Sect. 4.6.

2.2 Unsupervised graph-level representation learning

In recent years, GNN related models [32, 34, 61] have shown state-of-the-art performance in many graph data-related tasks such as nodes classification [23, 62] and graph classification [24, 36, 37, 63]. A number of graph representation learning methods have been proposed to handle the graph/node classification and node clustering tasks. For example, [55] proposed to learn low-dimensional mapping for nodes that maximally preserves the neighborhood information of nodes. [64] proposed to learn node representations for node classification via maximizing the mutual information between the patch representations and summarized graph representations. Similarly, [37] utilized the mutual information maximization strategy and GIN [24] to learn graph representations for graph-level classifications. [65, 66] took inspiration from the self-supervised learning to augment the graph data to construct positive/negative pairs, thereby learning effective graph representations with contrastive learning strategy [67].

It should be pointed out that existing graph representation learning methods rarely investigate the graph-level clustering task, as it is far more difficult than graph classification or node clustering. An intuitive strategy is to perform k-means [54] or spectral clustering [41] on the learned graph-level representations given by those methods. Nevertheless, the clustering performance is not desirable as can be observed in Sect. 4.4, because the representations learned by those methods are not guaranteed to be suitable or effective for graph-level clustering. Therefore, we present our DGLC method to investigate the way to learn clustering-oriented graph-level representations, of which the learning is guided by an explicit clustering objective.

3 Methodology

3.1 Problem formulation

Given a set of n graphs, i.e., $\mathcal{G} := \{G_1, G_2, \ldots, G_n\}$, where the i-th graph $G_i = (V_i, E_i)$ has node features $\mathbf{X}_i = \{\mathbf{x}_v^{(i)}\}_{v \in V_i}$ and $\mathcal{X} := \{\mathbf{X}_1, \mathbf{X}_2, \ldots, \mathbf{X}_n\}$. The graph-level clustering aims to partition the set $\mathcal{G}$ into a few non-overlapped groups, i.e., $\mathcal{G} = \mathcal{G}^{(1)} \cup \mathcal{G}^{(2)} \cup \cdots \mathcal{G}^{(c)}$ and $\mathcal{G}^{(i)} \cap \mathcal{G}^{(j)} = \emptyset$ for any $i \neq j$, such that the graphs in the same group are similar while the graphs in different groups are dissimilar, without using any label information.

Since the original graph data may not have graph-level feature vectors or they often contain redundant and distracting information, a more effective way is to perform clustering in a latent space given by some representation learning methods. Nevertheless, the two-step models discussed in Sect. 2.2, i.e., those based on graph kernels and graph-level representation learning, cannot guarantee to learn clustering-oriented graph representations because they are not optimized specifically for graph-level clustering tasks. Therefore, we propose to learn latent representations and conduct clustering simultaneously, where representation learning and clustering facilitate each other. We formalize the objective function for graph-level clustering as follows:

$$\mathcal{L}(\phi, \theta) := L_r(g_\phi(\mathcal{X}, \mathcal{G}), \mathcal{X}, \mathcal{G}) + L_{c|\theta}(g_\phi(\mathcal{X}, \mathcal{G})). \tag{1}$$

In (1), L_r denotes the representation learning objective that aims to map the input data $\mathcal{X}, \mathcal{G}$ into a latent space via a deep graph neural network with parameters ϕ. $L_{c|\theta}$ denotes the clustering objective on the representations $g_\phi(\mathcal{X}, \mathcal{G})$ and is associated with a deep neural network with parameters θ that may also contain the cluster centers or assignments. Note that there could be a trade-off parameter between L_r and $L_{c|\theta}$, but we just ignore it for convenience. We see that the objective $\mathcal{L}(\phi, \theta)$ does not only learn cluster-oriented representations, but also directly produces clustering results. So there is no need to perform k-means or spectral clustering after the pure representation learning like the two-step models.

3.2 Graph-level representation learning module

To learn effective representations of the graphs, we take advantage of GNN [23, 24, 32]. GNN leverages node information and structural information to learn representations for nodes or graphs. GNN aggregates the neighboring information of each node to itself iteratively; thus, the learned features could capture both the inherent node information and its neighbors' information. Specifically, the learned feature $\mathbf{h}_v$ for node v in the k-th layer can be formulated as follows:

$$\begin{aligned}\mathbf{h}_v^{(k)} &= \mathrm{COMBINE}^{(k)}\left(\mathbf{h}_v^{(k-1)}, \mathbf{a}_v^{(k)}\right)\\ &= \mathrm{COMBINE}^{(k)}\left(\mathbf{h}_v^{(k-1)}, \mathrm{AGGREGATE}^{(k)}(\{\mathbf{h}_u^{(k-1)} : u \in \mathcal{N}(v)\})\right),\end{aligned} \tag{2}$$

where $\mathrm{AGGREGATE}^{(k)}(\{\mathbf{h}_u^{(k-1)} : u \in \mathcal{N}(v)\}) = \sum_{u \in \mathcal{N}(v)} \mathbf{h}_u^{(k-1)}$ denotes the aggregated operation of neighbor features of node v, and $\mathcal{N}(v)$ is the neighborhood set of node v. Thus, $\mathbf{a}_v^{(k)}$ denotes the aggregated neighbor features in the k-th layer. $\mathrm{COMBINE}^{(k)}\left(\mathbf{h}_v^{(k-1)}, \mathbf{a}_v^{(k)}\right) = \sigma(\mathbf{W}^{(k)} \cdot (\mathbf{h}_v^{(k-1)} + \mathbf{a}_v^{(k)}) + \mathbf{b}^{(k)})$ the denotes combine operation to obtain the updated feature of node v in the k-th layer, where $\sigma(\cdot)$, $\mathbf{W}^{(k)}$, and $\mathbf{b}^{(k)}$ indicate the activation function (e.g., ReLU), weight matrix, and bias in the k-th layer. Particularly, the initial representation $\mathbf{h}_v^{(0)}$ is set as the node features of v, i.e., $\mathbf{x}_v$. It is worth noting that more global information could be obtained as the layer deepens, while some more generalized information would be possessed in the earlier layers [24]. Therefore, considering the information from various depths of the network would help us get more powerful representations for graph-level clustering tasks. Following the idea, we concatenate the representation learned at each layer as:

$$\mathbf{h}_\phi^i = \mathrm{CONCAT}\left(\{\mathbf{h}_i^{(k)}\}_{k=1}^K)\right), \tag{3}$$

where $\mathbf{h}_\phi^i$ is concatenated representation for node i, and $\mathbf{h}_i^{(k)}$ is the representation learned in k-th layer. After that, we can utilize a READOUT function to obtain the graph-level representation, i.e.,

$$\mathbf{H}_\phi(G_j) = \mathrm{READOUT}(\{\mathbf{h}_\phi^i\}_{i=1}^{|G_j|}), \tag{4}$$

where $|G_j|$ denotes the number of nodes in G_j. Therefore, for the given graph dataset $\bar{G} := \{G_j \in \mathcal{G}\}_{j=1}^{n_b}$ in a batch, $\mathbf{H}_\phi(\bar{G}) \in \mathbb{R}^{n_b \times K d_h}$ can be regarded as the learned graph-level representations, where n_b is number of graphs in a batch, d_h is the dimension of each hidden layer of GNN and K is the number of GNN layers. Note that we use the sum readout strategy in this work.

As graph-level clustering is an unsupervised learning task, it is important to learn more representative features in an unsupervised manner. We follow [37, 68] to achieve this by maximizing the mutual information between the representations of entire graphs and sub-structures, since it has been demonstrated as a powerful unsupervised graph representation learning technique. Specifically, for the given graph datasets in a batch $\bar{G}$ that follows an empirical probability distribution $\mathbb{P}$ on the original data space, the estimator $I_{\phi,\psi}$ of the mutual information (MI) over the global and local pairs is defined as follows:

$$\hat{\phi}, \hat{\psi} = \arg\max_{\phi,\psi} \sum_{\bar{G} \subseteq \mathcal{G}} \frac{1}{|\bar{G}|} \sum_{i \in \bar{G}} I_{\phi,\psi}(\mathbf{h}_\phi^i(\bar{G}); \mathbf{H}_\phi(\bar{G})) \triangleq -L_{r|\phi,\psi}, \tag{5}$$

where $|\bar{G}|$ is the number of nodes in $\bar{G}$, i denotes a single node in $\bar{G}$, $I_{\phi,\psi}$ can be parameterized by a discriminator network T with parameter ψ. By using Jensen-Shannon MI estimator [69], $I_{\phi,\psi}$ can be formulated as:

$$\begin{aligned} I_{\phi,\psi}\left(\mathbf{h}^i_\phi(\bar{G});\mathbf{H}_\phi(\bar{G})\right) :& \\ &= \mathbb{E}_{\mathbb{P}}\left[-\mathrm{sp}(-T_{\phi,\psi}\left(\mathbf{h}^i_\phi(s);\mathbf{H}_\phi(s)\right)\right)\Big] \\ &\quad - \mathbb{E}_{\mathbb{P}\times\tilde{\mathbb{P}}}\left[\mathrm{sp}\left(T_{\phi,\psi}(\mathbf{h}^i_\phi(s');\mathbf{H}_\phi(s))\right)\right], \end{aligned} \tag{6}$$

where $\mathbb{P}$ denotes the distribution of graph set $\bar{G}$, s denotes the input (positive) sample, and s' denotes the negative sample from the distribution $\tilde{\mathbb{P}}$ that is identical to distribution $\mathbb{P}$. Particularly, the combinations of global (graph-level) and local (node-level) representations in a batch are used to produce negative samples. $\mathrm{sp}(y) = \log(1 + e^y)$ indicates the softplus function. Note that we maximize the MI between graph-level and node-level representations, which facilitates graph-level representations to contain as much information as possible that is shared between node-level representations. It is intuitive that performing k-means or spectral clustering directly on the graph-level representations learned seems to be an applicable way, but it often tends to be a trivial solution because the representations learned in this way solely are not guaranteed to be applicable for the graph-level clustering task that we focus in this work.

3.3 End-to-end graph-level clustering module

To capture more suitable representations for graph-level clustering, we attempt to learn cluster-oriented representations by introducing an explicit clustering objective. Specifically, we propose a clustering network connected with graph-level features in the representation learning network described above. Then, the graph-level features will be projected to the cluster embedding in the low-dimensional latent space, which can be formalized as follows:

$$\mathbf{z}_j = f_\theta(\mathbf{H}_\phi(G_j)), \tag{7}$$

where $\mathbf{z}_j$ denotes the learned cluster embedding for graph G_j, and f_θ is the MLP-based clustering projector with network parameter θ. Let $\mathbf{Z}_{\phi,\theta}(\bar{G}) \in \mathbb{R}^{d_z \times n_b}$ be the cluster embeddings in a batch, where d_z is the dimension of cluster embedding layer. Subsequently, we take inspiration from [70, 71] to define the graph-level cluster assignment distribution Q based on $\mathbf{Z}_{\phi,\theta}(\bar{G})$ as follows:

$$q_{jt|\phi,\theta} = \frac{(1 + \|\mathbf{z}_j - \boldsymbol{\mu}_t\|^2)^{-1}}{\sum_{t=1}^{c}(1 + \|\mathbf{z}_j - \boldsymbol{\mu}_t\|^2)^{-1}}, \tag{8}$$

where $\mathbf{z}_j$ is the j-th column of $\mathbf{Z}_{\phi,\theta}(\bar{G})$, c is the number of clusters, $\boldsymbol{\mu}_t$ is the t-th cluster center that can be initialized by k-means, and $q_{jt|\phi,\theta}$ is the graph-level cluster assignment indicating the probability that graph G_j belongs to cluster t. Next, we can further define an auxiliary refined cluster assignment distribution P to emphasize those assignments with high confidence in Q as follows:

$$p_{jt} = \frac{q^2_{jt|\phi,\theta} / \sum_{j=1}^{n_b} q_{jt|\phi,\theta}}{\sum_{t=1}^{c}(q^2_{jt|\phi,\theta} / \sum_{j=1}^{n_b} q_{jt|\phi,\theta})}, \tag{9}$$

where P encourages a more pronounced gap between assignments with high and low probability in Q and can be regarded as pseudo-labels for guiding the optimization of Q. Therefore, we can define the clustering objective by minimizing the KL-divergence between P and Q as follows:

$$L_{c|\phi,\theta} = KL(P\|Q) = \sum_{j=1}^{n_b}\sum_{t=1}^{c} p_{jt}\log\frac{p_{jt}}{q_{jt|\phi,\theta}}. \tag{10}$$

$L_{c|\theta}$ aims to force Q to approximate P, i.e., to let P guide the optimization of Q so that the high confident assignment can be emphasized, which can also be regarded as a self-training strategy. By jointly optimizing Eqs. 5 and 10, we can construct an end-to-end deep graph-level clustering framework that simultaneously implements graph-level representation learning and clustering. The overall objective of DGLC in terms of minibatch optimization is as follows:

$$\begin{aligned} L_{\text{batch}}(\phi,\psi,\theta) = & \underbrace{-\frac{1}{|\bar{G}|}\sum_{i\in\bar{G}} I_{\phi,\psi}(\mathbf{h}^i_\phi(\bar{G});\mathbf{H}_\phi(\bar{G}))}_{L_{r|\phi,\psi}} \\ & + \underbrace{\sum_{j=1}^{n_b}\sum_{t=1}^{c} p_{jt}\log\frac{p_{jt}}{q_{jt|\phi,\theta}}}_{L_{c|\phi,\theta}}. \end{aligned} \tag{11}$$

where $|\bar{G}|$ and n_b denote the number of nodes and graphs in a batch. Besides, $\mathbf{h}^i_\phi(\bar{G})$ and $\mathbf{H}_\phi(\bar{G})$ indicate the learned node-level and graph-level feature matrices, respectively.

4 Experiments

In this section, we evaluate the proposed method in comparison with several state-of-the-art competitors in graph-level clustering tasks. We first introduce the datasets and baseline methods used in the experiment and describe the detailed settings of the network and parameters. Then, we demonstrate the effectiveness of our method through comprehensive experimental analysis.

4.1 Dataset description and baseline methods

4.1.1 Dataset

We use six well-known graph datasets in the experiment, including MUTAG,[1] PTC-MR,[2] PTC-MM,[3] BZR,[4] ENZYMES,[5] COX2.[6] We provide detailed information of six graph datasets used in our experiment here:

- **MUTAG** is a compound dataset that contains 188 compounds, which are grouped into 2 categories based on their mutagenic effect on a bacterium. Note molecules possess a natural graph structure, where they are expressed by an average of 17.93 nodes (for atoms) and 19.79 edges (for chemical bonds).
- **PTC-MR** and **PTC-MM** are the subset of the PTC dataset, which is a compound dataset that is divided into 2 categories based on the carcinogenicity of rodents. Note that PTC-MR contains 344 compounds with an average of 14.29 nodes and 14.69 edges, while PTC-MM contains 336 compounds with an average of 13.97 nodes and 14.32 edges, respectively.
- **BZR** is the ligand dataset for benzodiazepine receptors, which are divided into 2 classes according to the activity and inactivity of compounds. Note that BZR contains 405 graphs in total with an average of 35.75 nodes and 38.36 edges per graph.
- **ENZYMES** contains 600 protein data for 6 classes of enzymes, with 100 proteins per class. Each protein data can be represented as a graph with an average of 32.63 nodes and 62.14 edges.
- **COX2** consists of 467 inhibitors for cyclooxygenase-2 and are divided into 2 classes based on whether the compounds are active or inactive. Note that each graph in this dataset is with an average of 41.22 nodes and 43.45 edges.

We summarize the information of each dataset in Table 2

4.1.2 Baseline methods

We compare the proposed DGLC method with 10 state-of-the-art graph-level clustering approaches, i.e.:

- **Graph kernel:** Random walk kernel (RW) [30], Weisfeiler-Lehman kernel (WL) [49], Optimal assignment-based WL kernel (WL-OA) [72], Shortest-path kernel (SP) [58], Lovasz-theta kernel (LT) [73], and Graphlet kernel (GK) [57].
- **Unsupervised graph-level representation learning:** including InfoGraph [37], Gromov-Wasserstein factorization (GWF) [74], Graph contrastive learning (GraphCL) [65], and Joint augmentation optimization (JOAO) [66].

Note that we evaluate the clustering performance of all comparative methods via k-means clustering [54] and spectral clustering [41], more details about the experimental settings refer to Sect. 4.2.

4.1.3 Evaluation metrics

We introduce three clustering metrics used in this paper, with y_j and $\hat{y}_j$ denoting the true labels and the predicted labels for graph G_j respectively.

- **Clustering accuracy (ACC):** ACC is expressed as the comparison of the true labels and predicted labels leveraged on sample size n, which is defined as follows:

$$\mathrm{ACC} = \frac{\sum_{i=1}^{n} \delta(y_j, \hat{y}_j)}{n}, \text{ where } \delta(x, y) = \left\{ \begin{array}{ll} 1 & \text{if } x = y \\ 0 & \text{otherwise} \end{array} \right\} \tag{12}$$

- **Normalized mutual information (NMI):** NMI score scales the mutual information scores by some generalized mean of entropy of true label set Ω and cluster label set C. It can be formalized as follows:

$$\mathrm{NMI}(\Omega, C) = \frac{I(\Omega; C)}{(H(\Omega) + H(C))/2} \tag{13}$$

where $I(\Omega; C) = H(\Omega) + H(C) - H(\Omega, C)$ denotes the mutual information between Ω and C, and $H(\cdot)$ is the information entropy.

- **Adjusted rand index (ARI):** ARI score is an adjusted score of Rand index (RI) for chance. RI is also a similarity measure by considering all pairs of samples and counting pairs that are assigned in the same or different clusters in the predicted and true labels. ARI can be formalized as follows:

$$\begin{aligned} \mathrm{ARI} &= \frac{(\mathrm{RI} - \text{Expected RI})}{(\max(\mathrm{RI}) - \text{Expected RI})} \\ &= \frac{\sum_{ij}\binom{n_{ij}}{2} - \left[\sum_i \binom{a_i}{2} \sum_j \binom{b_j}{2}\right] / \binom{n}{2}}{\frac{1}{2}\left[\sum_i \binom{a_i}{2} + \sum_j \binom{b_j}{2}\right] - \left[\sum_i \binom{a_i}{2} \sum_j \binom{b_j}{2}\right] / \binom{n}{2}} \end{aligned} \tag{14}$$

where $a_i = \sum_{j=1}^{r} n_{ij}$, $b_i = \sum_{i=1}^{s} n_{ij}$, n_{ij} denotes an entry from the contingency table of cluster i and class j, r and s are numbers of clusters and classes.

[1] https://www.chrsmrrs.com/graphkerneldatasets/MUTAG.zip.
[2] https://www.chrsmrrs.com/graphkerneldatasets/PTC-MR.zip.
[3] https://www.chrsmrrs.com/graphkerneldatasets/PTC-MM.zip.
[4] https://www.chrsmrrs.com/graphkerneldatasets/BZR.zip.
[5] http://www.chrsmrrs.com/graphkerneldatasets/ENZYMES.zip.
[6] https://www.chrsmrrs.com/graphkerneldatasets/COX2.zip.

Table 2 Information of the six benchmark datasets

Dataset name	Number of graphs	Range of nodes	Average nodes	Range of edges	Average edges	Classes
MUTAG	188	[10–28]	17.93	[20–66]	19.79	2
PTC-MR	344	[2–64]	14.29	[2–142]	14.69	2
PTC-MM	336	[2–64]	13.97	[2–142]	14.32	2
BZR	405	[13–57]	35.75	[26–120]	38.36	2
ENZYMES	600	[2–126]	32.63	[2–298]	62.14	6
COX2	467	[32–56]	41.22	[68–118]	43.45	2

Note that ACC and NMI range from [0, 1], while ARI ranges from $[-1, 1]$. The higher values of ACC, NMI, and ARI represent better clustering performance.

4.2 Experimental settings

For the graph kernel methods we compared with, they are all normalized with the base graph kernel to be Vertex Histogram kernel if needed. We directly perform spectral clustering [41] on the similarity matrices produced by them to obtain the clustering results. Note that we also include the *k*-means [54] performance of several graph kernels in Sect. 4.7. While for the unsupervised graph-level representation learning methods, e.g., InfoGraph, GraphCL, JOAO, we perform *k*-means [54] and spectral clustering on the learned graph-level representations. Particularly, for GWF [74] we not only follow the original paper to perform *k*-means, but also perform spectral clustering to evaluate its clustering performance.

To provide a fair comparison in our experiment, we use exactly the same network architecture as our competitors of unsupervised graph representation learning [37, 65, 66], i.e., utilizing the Graph isomorphism network (GIN) [24] as the backbone GNN. The cluster projector is constructed with a two-layer MLP-based fully connected network. We use Adam as the optimizer, the learning rate is chosen from $[10^{-3}, 10^{-5}]$, the batch size is set to 128 and the total running epoch is set to 20. Moreover, there are three important hyper-parameters in our method, i.e., the layer numbers of GNN, the hidden dimension d_h of each GNN layer, and the dimension d_z of the clustering layer. We evaluate the influence of different values of them on the graph-level clustering performance in Sect. 4.5 due to the limitation of the paper length.

To evaluate the clustering performance, we consider three popular metrics including clustering accuracy (ACC), normalized mutual information (NMI), and adjusted rand index (ARI). We utilize Pytorch Geometric [75] and GraKeL [76] libraries to implement our method and other baseline methods. Note that we run all experiments 10 times with NVIDIA Tesla A100 GPU and AMD EPYC 7532 CPU, and report their means and standard deviations.

4.3 Experimental results

We compare the proposed DGLC method with 13 baselines and state-of-the-art methods on the six popular benchmarks. The experimental results are shown in Tables 3, 4 and 5, from which we have the following observations.

First, graph kernel-based graph-level clustering approaches are effective on only a few datasets, while achieving mediocre clustering performances on most datasets. For example, the RW kernel performs well on MUTAG and PTC-MR, but mediocre on PTC-MM and BZR. While the opposite results are observed on the LT kernel, this is because graph kernels are mainly based on hand-crafted design and are not suitable for arbitrary datasets in practice. Second, the unsupervised graph representation learning methods show potential in handling graph-level clustering. For example, JOAO obtains encouraging performance on MUTAG, BZR, and COX2. GWF achieves state-of-the-art performance on ENZYMES. Although such methods achieve promising graph-level clustering performance in many cases, they still suffer from the undesirable graph-level representations learned for clustering, i.e., their representation learning does not explicitly optimize for the clustering task. Third, the proposed DGLC method outperforms both types of the above solutions by a large margin in most cases. For example, DGLC outperforms the runner-up with 5.48% and 13.27% advantages on MUTAG in terms of ACC and ARI, and with 1.47%, 5.66% and 14.91% advantages on BZR in terms of ACC, NMI, and ARI. This fully demonstrates the effectiveness of our method. Compared with graph kernel-based approaches, DGLC is more general for different types of graph data. Compared with the latest unsupervised graph representation learning approaches, DGLC has a clear clustering objective in the optimization and thus tends to learn clustering-oriented graph-level representations and achieves state-of-the-art performance.

Table 3 Clustering performance (ACC, NMI, ARI) on MUTAG and PTC-MR

Method	MUTAG			PTC-MR		
	ACC	NMI	ARI	ACC	NMI	ARI
Graph kernel followed by spectral clustering (SC)						
RW [30]+SC	77.65±0.00	30.81±0.00	30.26±0.00	56.98±0.00	0.63±0.00	1.25±0.00
WL [49]+SC	73.40±0.00	14.50±0.00	21.20±0.00	52.91±0.00	0.23±0.00	0.05±0.00
WL-OA [72]+SC	67.55±0.00	19.64±0.00	11.40±0.00	59.30±0.00	1.77±0.00	2.95±0.00
SP [58]+SC	72.87±0.00	10.24±0.00	15.95±0.00	56.69±0.00	1.04±0.00	0.50±0.00
LT [73]+SC	56.60±4.88	3.09±1.38	−0.62±0.63	55.17±1.32	0.40±0.65	0.19±0.52
GK [57]+SC	67.02±0.00	1.74±0.00	1.04±0.00	56.40±0.00	1.32±0.00	0.31±0.00
Unsupervised graph representation learning followed by k-means (KM) and SC						
InfoGraph [37]+KM	77.95±1.41	35.22±3.47	30.95±3.03	54.79±0.68	0.49±0.35	0.28±0.21
InfoGraph [37]+SC	72.58±4.83	28.68±4.93	19.85±5.91	56.10±0.33	1.50±0.26	0.20±0.13
GWF [74]+KM	66.94±7.68	12.46±9.31	13.32±10.53	56.33±3.52	1.09±0.88	1.65±1.50
GWF [74]+SC	73.92±4.30	18.35±3.85	24.48±4.69	55.32±4.03	0.89±0.84	1.49±1.44
GraphCL [65]+KM	77.07±1.21	35.69±2.83	28.99±2.65	54.33±0.76	1.15±0.55	0.16±0.29
GraphCL [65]+SC	73.22±2.66	32.19±2.05	23.44±2.45	56.13±0.42	1.31±0.30	1.17±0.24
JOAO [66]+KM	79.20±0.72	**36.32±3.03**	33.74±1.65	56.39±0.18	0.53±0.21	0.41±0.01
JOAO [66]+SC	70.72±2.85	27.73±0.23	17.12±2.03	56.16±0.22	1.03±0.33	0.19±0.11
DGLC(Ours)	**84.68±0.89**	35.75±2.51	**47.01±2.64**	**60.93±0.57**	**2.98±0.43**	**4.29±0.52**

The best result is highlighted in bold

Table 4 Clustering performance (ACC, NMI, ARI) on PTC-MM and BZR

Method	PTC-MM			BZR		
	ACC	NMI	ARI	ACC	NMI	ARI
Graph kernel followed by spectral clustering (SC)						
RW [30]+SC	60.71±0.00	0.97±0.00	2.91±0.00	64.69±0.00	0.00±0.00	−0.15±0.00
WL [49]+SC	62.20±0.00	1.50±0.00	3.87±0.00	75.56±0.00	0.50±0.00	3.76±0.00
WL-OA [72]+SC	63.39±0.00	4.59±0.00	2.26±0.00	69.63±0.00	5.60±0.00	−8.67±0.00
SP [58]+SC	62.20±0.00	1.63±0.00	0.73±0.00	79.51±0.00	4.13±0.00	3.97±0.00
LT [73]+SC	61.19±0.88	0.73±0.55	1.09±1.06	78.35±0.35	0.69±0.28	1.12±1.03
GK [57]+SC	62.20±0.00	1.63±0.00	0.73±0.00	61.23±3.36	1.06±1.21	3.13±3.74
Unsupervised graph representation learning followed by k -means (KM) and SC						
InfoGraph [37]+KM	61.48±1.03	2.35±0.83	3.61±1.45	63.62±2.41	1.59±0.95	2.39±1.44
InfoGraph [37]+SC	61.96±1.53	2.12±0.99	4.55±0.83	73.53±2.66	3.66±2.52	5.04±3.12
GWF [74]+KM	53.37±3.18	0.30±0.37	0.38±1.09	53.00±0.31	3.42±0.45	−0.76±0.05
GWF [74]+SC	53.02±1.66	0.36±0.28	0.21±0.09	52.76±0.80	3.47±1.16	−0.71±0.32
GraphCL [65]+KM	58.93±0.74	0.27±0.15	0.60±0.14	71.43±4.09	1.04±0.77	3.07±1.03
GraphCL [65]+SC	62.09±0.56	2.14±0.43	3.36±0.87	72.88±1.66	1.90±0.38	3.47±0.59
JOAO [66]+KM	59.04±0.52	0.21±0.14	0.98±0.41	72.64±4.26	1.37±1.14	4.01±3.39
JOAO [66]+SC	62.41±0.80	2.00±0.78	4.28±1.34	72.98±1.59	2.75±1.30	5.62±3.74
DGLC(Ours)	**63.30±0.81**	**2.70±0.45**	**5.53±0.61**	**80.98±0.60**	**9.79±0.92**	**20.53±1.84**

The best result is highlighted in bold

4.4 Qualitative study

In this section, we conduct a qualitative study to provide a visual comparison of graph-level clustering. Specifically, we compare our method with several state-of-the-art unsupervised graph representation learning methods including InfoGraph, GWF, GraphCL, and JOAO by utilizing t-SNE [70] and visualize their learned graph-level representations on MUTAG and ENZYMES. The visualization results are shown in Fig. 1.

Table 5 Clustering performance (ACC, NMI, ARI) on ENZYMES and COX2

Method	ENZYMES			COX2		
	ACC	NMI	ARI	ACC	NMI	ARI
Graph kernel followed by spectral clustering (SC)						
RW [30]+SC	17.00±0.00	0.66±0.00	0.25±0.00	51.31±0.00	0.70±0.00	−0.92±0.00
WL [49]+SC	21.00±0.00	3.09±0.00	1.48±0.00	50.54±0.00	0.51±0.00	−0.40±0.00
WL-OA [72]+SC	20.00±0.00	1.35±0.00	0.32±0.00	50.75±0.00	0.51±0.00	−0.37±0.00
SP [58]+SC	22.00±0.00	2.57±0.00	1.69±0.00	52.03±0.00	0.13±0.00	0.01±0.00
LT [73]+SC	17.00±0.09	0.42±0.11	0.00±0.00	77.52±0.59	0.26±0.34	0.17±0.71
GK [57]+SC	17.07±0.13	0.80±0.25	0.00±0.00	66.17±0.00	0.02±0.00	0.08±0.17
Unsupervised graph representation learning followed by k -means (KM) and SC						
InfoGraph [37]+KM	22.06±0.98	2.40±0.45	1.25±0.52	56.74±3.04	3.30±0.60	0.17±0.10
InfoGraph [37]+SC	23.75±0.50	4.64±0.65	2.23±0.41	70.37±2.01	**3.56± 0.99**	1.92±1.67
GWF [74]+KM	**28.55±0.20**	6.02±0.55	**3.16± 0.20**	57.60±4.11	1.50±0.13	2.08±1.80
GWF [74]+SC	25.66±1.57	5.24±1.28	1.78±0.61	58.83±4.46	1.16±0.41	1.45±1.21
GraphCL [65]+KM	21.50±0.22	1.55±0.12	0.90±0.09	68.88±0.59	1.05±0.21	0.44±0.57
GraphCL [65]+SC	25.28±0.28	4.75±0.36	2.03±0.26	75.01±2.12	1.24±0.37	2.39±2.28
JOAO [66]+KM	21.66±0.37	1.60±0.01	0.94±0.02	70.56±2.03	1.19±0.34	0.44±0.43
JOAO [66]+SC	24.65±0.44	4.85±0.37	2.07±0.18	76.46±0.61	1.43±0.77	2.35±2.49
DGLC(Ours)	27.08±1.49	**6.39±1.09**	2.86±0.80	**78.28±0.17**	2.38±0.99	**6.79±3.37**

The best result is highlighted in bold

We can observe that compared with other methods, DGLC explicitly reveals a more compact intra-class structure and more distinct inter-class discrepancy. For example, the learned representations of the two classes in MUTAG are more separated in our method compared to others. Besides, we can find that InfoGraph, GraphCL, and JOAO fail to capture good clustering structures for ENZYMES, while GWF and ours do. In general, the visualization results of the learned graph-level representations also support the effectiveness of our method.

4.5 Parameter sensitivity analysis and ablation study

To evaluate the robustness of DGLC and the effectiveness of each component, we conduct the parameter sensitivity analysis and ablation study.

4.5.1 Parameter sensitivity analysis

We analyze the sensitivity of DGLC to the hyperparameters, i.e., the hidden dimension d_h of GNN layers, the embedding dimension d_z of the clustering layer, and the

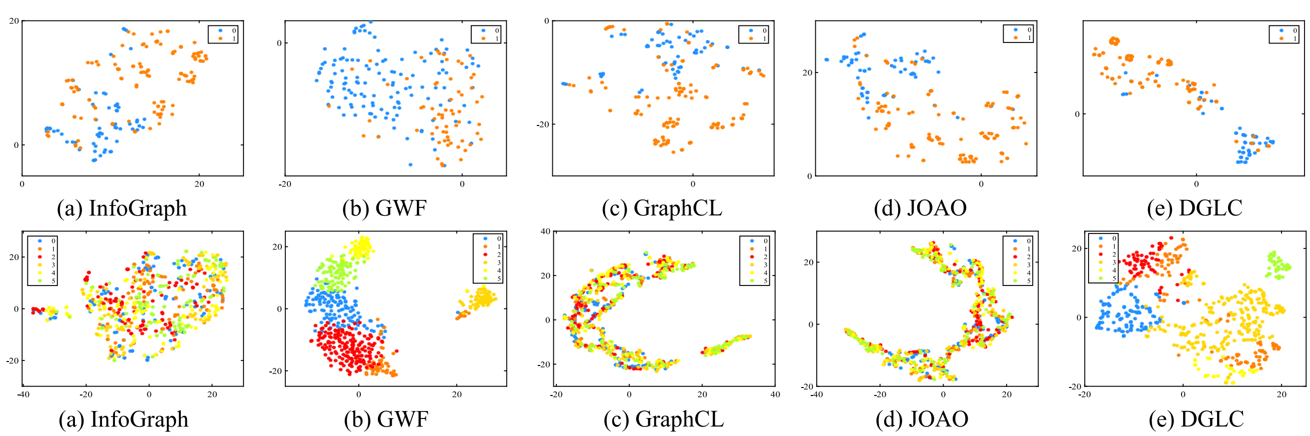

Fig. 1 t-SNE visualization of the learned graph-level representations of our methods and other unsupervised graph representation learning methods. The first row is the visualization for MUTAG, while the second row is for ENZYMES

number of GNN layers. Here, we take MUTAG and PTC-MR datasets as examples to evaluate the influence of the change of d_h and d_z values. Specifically, we select the values of d_h in $[16, 32, \ldots, 256]$ and d_z in $[5, 10, \ldots, 30]$, and the results are shown in Fig. 2.

We can observe that the ACC on both datasets is relatively stable, showing little fluctuation when the values of parameters vary in a wide range. In contrast, NMI and ARI are of high performance when the selection of parameters is moderate. In general, DGLC shows robust performance against the two parameters. Nevertheless, we recommend choosing d_z from 10 to 25 and d_h from 32 to 128 to obtain better clustering performance in practice. Except for the ones mentioned above, we further conduct the sensitivity analysis on the number of GNN hidden layers on three datasets (MUTAG, PTC-MR, and BZR). We vary the number of GNN hidden layers in $[2, 3, \ldots, 10]$. The experimental results are shown in Fig. 3. It could be seen that PTC-MR is quite stable for all three metrics. For MUTAG and BZR, DGLC shows better performance when setting the number of GNN hidden layers to 4 and 5. In general, DGLC obtains relatively stable performance at different numbers of GNN layers, despite fluctuations at some specific fetch values.

4.5.2 Ablation study

In this section, we conduct experiments to evaluate the influence of each proposed strategy on our method. Specifically, we construct four degradation models of our method by, respectively, removing some components of it. There are:

- DGLC_{d1}: We remove the clustering loss and joint training strategy of DGLC and evaluate the model by performing k-means on the learned graph-level representations, i.e., the model can be regarded as InfoGraph in this way.
- DGLC_{d2}: We keep the clustering loss and joint training strategy while directly using k-means to produce the clustering results instead of producing the clustering labels with the cluster label assignment Q.
- DGLC_{d3}: We degrade DGLC as a two-stage model, i.e., we train the model by, respectively, optimizing the graph representation learning objective and clustering objective. The clustering results are still obtained from the graph-level cluster assignment Q in the second training stage.

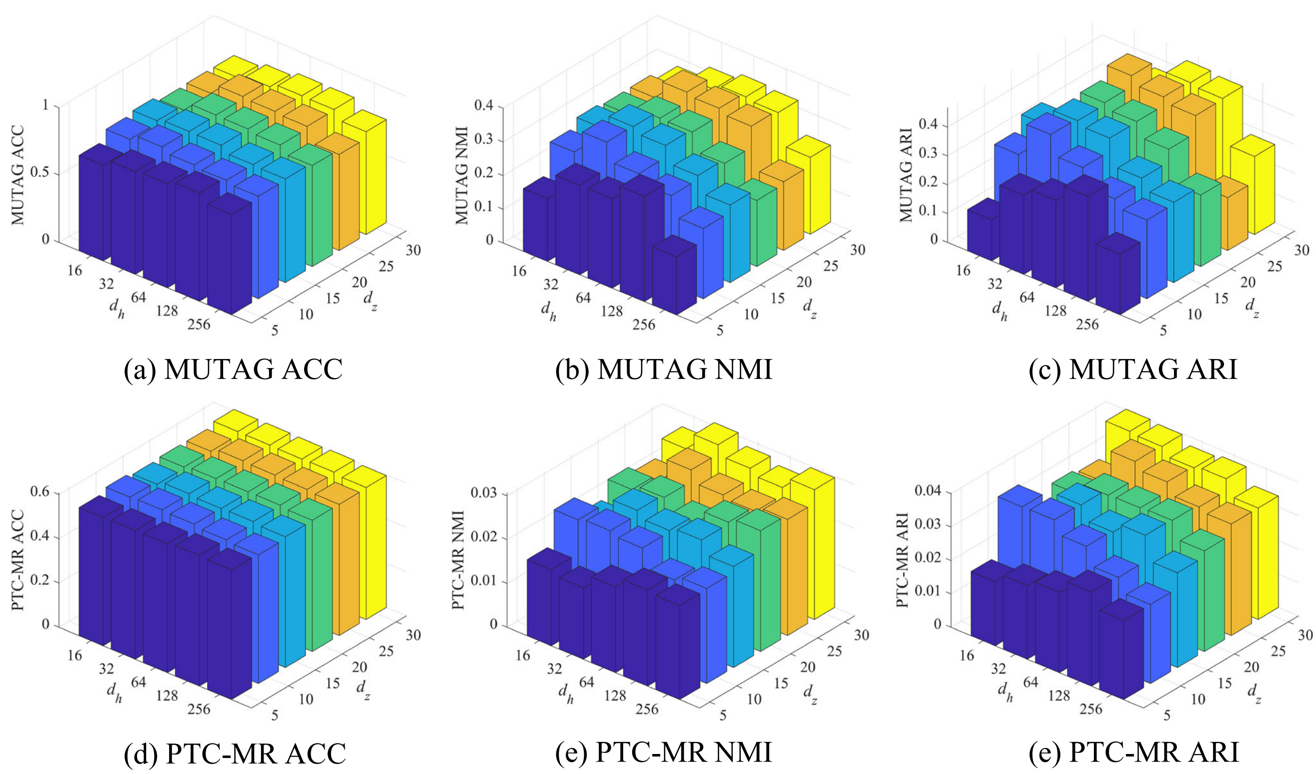

(a) MUTAG ACC (b) MUTAG NMI (c) MUTAG ARI

(d) PTC-MR ACC (e) PTC-MR NMI (e) PTC-MR ARI

Fig. 2 Sensitivity analysis of ACC, NMI, and ARI regarding the dimension d_h of GNN hidden layers and the embedding dimension d_z of clustering layer on MUTAG and PTC-MR datasets. It can be observed that all three metrics, especially ACC, show relative robustness against the variation of the hyper-parameter values

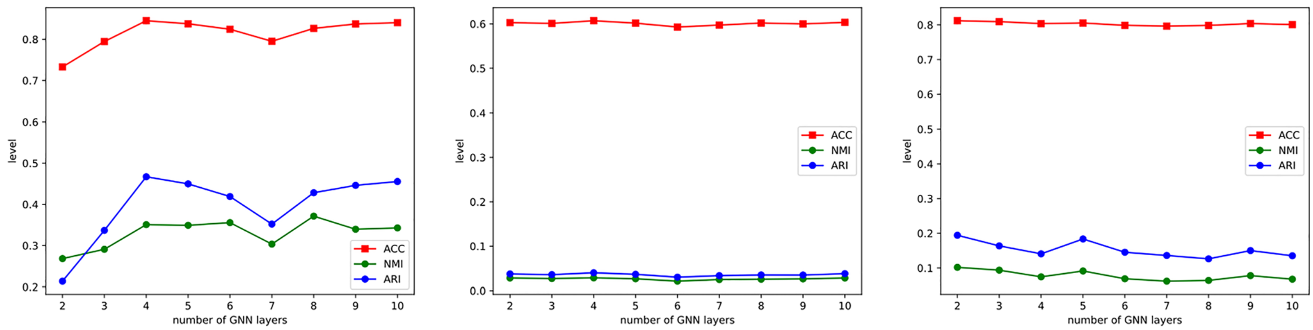

(a) MUTAG (b) PTC-MR (c) BZR

Fig. 3 Sensitivity analysis of ACC, NMI, and ARI regarding the number of GNN hidden layers on MUTAG, PTC-MR, and BZR datasets

We run experiments on MUTAG and BZR to evaluate their performance. Table 6 summarizes the experimental results, from which we have the following observations:

- Both DGLC$_{d2}$ and DGLC$_{d3}$ significantly outperform DGLC$_{d1}$, which fully suggests that learning clustering-oriented representations would benefit graph-level clustering.
- Producing clustering results from the graph-level cluster assignment Q is more reasonable as the clustering performance degrades when directly performing k-means on the learned cluster embeddings.
- Joint training with representation learning and clustering objectives yields better clustering performance. For example, DGLC outperforms DGLC$_{d3}$ by 3.20%, 4.86%, and 8.67% in terms of ACC, NMI, and ARI on MUTAG.

4.6 Computational time comparison

In this section, we demonstrate the time efficiency of DGLC by comparing the running time with several graph kernels and unsupervised graph representation learning baselines. Specifically, for graph kernels, we select RW [30], WL [49], SP [58] and LT [73] as our competitors. For unsupervised graph representation learning methods, we select GWF [74] and InfoGraph [37]. Note that we run 20 epochs for GWF, InfoGraph and DGLC for fair comparison. Table 7 shows the running times of each method on six benchmark datasets used in this paper. We can see that RW, LT, and GWF are quite time-consuming, especially on datasets like ENZYMES and COX2 which contain numerous nodes and edges. In contrast, WL, SP, InfoGraph, and DGLC are much more efficient compared to them and have comparable time efficiency.

4.7 *k*-means performance of graph kernels

Here, we provide k-means performance of some Graph kernels, including, RW [30], WL [49], WL-OA [72], and SP [58]. The experimental results are shown in Tables 8, 9 and 10. From these tables, we can observe that the graph kernels plus k-mean exhibit moderate effectiveness and perform better on some datasets than the SC results shown in Tables 3, 4 and 5. However, the performance of the graph kernels plus k-means is still unsatisfactory, as it can be seen that the performance of the proposed DGLC method outperforms them significantly.

4.8 Experiment on large-scale dataset

To validate the effectiveness of the proposed method on large-scale graph datasets, we supplement two more datasets in our experiment. Specifically, we choose NCI1, NCI109, and COLLAB datasets to conduct an experiment, the detailed information of the three datasets is shown in

Table 6 Clustering performance (ACC, NMI, ARI) on MUTAG and BZR

Method	MUTAG			BZR		
	ACC	NMI	ARI	ACC	NMI	ARI
DGLC$_{d1}$	77.95±1.41	35.22±3.47	30.95±3.03	63.62±2.41	1.59±0.95	2.39±1.44
DGLC$_{d2}$	80.50±2.34	32.52±3.65	37.16±5.53	66.61±3.14	1.98±1.29	4.32±2.54
DGLC$_{d3}$	81.48±2.31	30.89±3.98	38.34±6.61	73.87±2.58	2.92±2.30	5.35±3.96
DGLC	**84.68±0.89**	**35.75 ±2.51**	**47.01±2.64**	**80.98±0.60**	**9.79±0.92**	**20.53±1.84**

The best result is highlighted in bold

Table 7 Running time comparison (in seconds) on the six benchmark graph datasets

Method	MUTAG	PTC-MR	BZR	PTC-MM	ENZYMES	COX2
RW [30]+SC	12.29	29.29	76.34	25.44	2346.51	2457.56
WL [49]+SC	2.19	4.97	9.57	7.15	13.43	10.65
SP [58]+SC	3.60	5.38	25.49	5.08	53.75	32.39
LT [73]+SC	88.28	160.86	860.70	552.66	9117.17	6016.26
InfoGraph [37]+KM	9.23	10.96	23.42	11.48	29.37	28.99
InfoGraph [37]+SC	35.96	96.60	165.48	101.2	313.70	300.84
GWF [74]+KM	477.48	830.26	2480.76	803.81	3668.92	2945.12
GWF [74]+SC	566.41	911.37	2591.73	896.44	3954.87	3132.67
DGLC	10.16	12.12	25.66	12.84	31.87	30.50

Table 8 Clustering performance (ACC, NMI, ARI) on MUTAG and PTC-MR

Method	MUTAG			PTC-MR		
	ACC	NMI	ARI	ACC	NMI	ARI
Graph kernel followed by *k*-means (KM)						
RW [30]+KM	77.66±0.00	30.82±0.00	30.26±0.00	51.16±0.00	0.19±0.00	−0.55±0.00
WL [49]+KM	73.94±0.00	15.51±0.00	22.25±0.00	57.56±0.00	1.10±0.00	1.89±0.00
WL-OA [72]+KM	73.94±0.00	16.92±0.00	22.42±0.00	55.81±0.00	0.59±0.00	0.99±0.00
SP [58]+KM	76.06±0.00	15.38±0.00	25.11±0.00	59.30±0.00	1.87±0.00	2.73±0.00
DGLC(Ours)	**84.68±0.89**	**35.75±2.51**	**47.01±2.64**	**60.93±0.57**	**2.98±0.43**	**4.29±0.52**

The best result is highlighted in bold

Table 9 Clustering performance (ACC, NMI, ARI) on PTC-MM and BZR

Method	PTC-MM			BZR		
	ACC	NMI	ARI	ACC	NMI	ARI
Graph kernel followed by *k*-means (KM)						
RW [30]+KM	55.06±0.00	0.02±0.00	0.00±0.00	58.52±0.00	0.19±0.00	−1.55±0.00
WL [49]+KM	58.63±0.00	0.82±0.00	2.15±0.00	68.15±0.00	0.98±0.00	5.17±0.00
WL-OA [72]+KM	58.04±0.00	0.81±0.00	1.93±0.00	67.90±0.00	2.17±0.00	−6.78±0.00
SP [58]+KM	61.01±0.00	0.85±0.00	2.67±0.00	65.43±0.00	0.27±0.00	2.36±0.00
DGLC(Ours)	**63.30±0.81**	**2.70±0.45**	**5.53±0.61**	**80.98±0.60**	**9.79±0.92**	**20.53±1.84**

The best result is highlighted in bold

Table 10 Clustering performance (ACC, NMI, ARI) on ENZYMES and COX2

Method	ENZYMES			COX2		
	ACC	NMI	ARI	ACC	NMI	ARI
Graph kernel followed by *k*-means (KM)						
RW [30]+KM	23.17±0.00	2.50±0.00	1.74±0.00	53.96±0.00	0.60±0.00	−1.68±0.00
WL [49]+KM	21.50±0.00	2.18±0.00	0.96±0.00	50.96±0.00	0.54±0.00	−0.33±0.00
WL-OA [72]+KM	20.83±0.00	1.68±0.00	0.55±0.00	50.75±0.00	0.51±0.00	−0.37±0.00
SP [58]+KM	22.17±0.00	2.79±0.00	1.70±0.00	52.03±0.00	0.13±0.00	0.01±0.00
DGLC(Ours)	**27.08±1.49**	**6.39±1.09**	**2.86± 0.80**	**78.28±0.17**	**2.38±0.99**	**6.79±3.37**

The best result is highlighted in bold

Table 11 Information of the three large-scale datasets

Dataset name	Number of graphs	Average nodes	Average edges	Classes
NCI1	4,110	29.87	32.30	2
NCI109	4,127	14.29	14.69	2
COLLAB	5,000	74.49	2457.78	3

Table 12 Clustering performance (ACC, NMI, ARI) on NCI1 and NCI109

Method	NCI1			NCI109		
	ACC	NMI	ARI	ACC	NMI	ARI
Graph kernel followed by spectral clustering (SC)						
RW [30]+SC	N/A	N/A	N/A	N/A	N/A	N/A
WL [49]+SC	50.05±0.00	0.00±0.00	0.00±0.00	50.39±0.00	0.01±0.00	0.00±0.00
SP [58]+SC	50.10±0.00	0.10±0.00	0.00±0.00	52.26±0.00	0.33±0.00	0.19±0.00
LT [73]+SC	N/A	N/A	N/A	50.47±0.29	0.01±0.01	−0.01±0.01
Unsupervised graph representation learning followed by k-means (KM) and SC						
InfoGraph [37]+KM	54.11±2.15	1.28±1.11	0.85±0.87	54.38±1.85	1.25±0.74	0.89±0.68
InfoGraph [37]+SC	54.87±1.68	0.93±0.56	1.04±0.76	54.67±1.93	1.08±0.52	1.00±0.80
GraphCL [65]+KM	55.37±1.66	0.47±0.28	0.99±0.82	55.37±1.68	1.79±0.93	2.11±1.44
GraphCL [65]+SC	55.93±1.24	0.61±0.63	1.08±0.79	56.29±2.24	2.12±1.16	**2.48 ±2.79**
JOAO [66]+KM	51.12±0.37	0.43±0.18	0.05±0.03	56.20±0.58	1.73±0.72	1.54±0.28
JOAO [66]+SC	51.48±2.98	0.88±1.22	0.40±1.17	56.30±0.85	**4.61±0.43**	1.81±0.44
DGLC(Ours)	**57.69±2.31**	**2.50±0.89**	**2.56±1.39**	**56.36±2.31**	1.94±0.89	1.81±1.38

The best result is highlighted in bold. N/A denotes the results are unavailable (out of memory or the running time over 24 h)

Table 13 Clustering performance (ACC, NMI, ARI) on COLLAB

Method	COLLAB		
	ACC	NMI	ARI
Graph kernel followed by spectral clustering (SC)			
RW [30]+SC	N/A	N/A	N/A
WL [49]+SC	53.20±0.00	1.96±0.00	0.53±0.00
SP [58]+SC	48.72±0.00	17.91±0.00	**13.93±0.00**
LT [73]+SC	N/A	N/A	N/A
Unsupervised graph representation learning followed by k-means (KM) and SC			
InfoGraph [37]+KM	59.64±1.78	14.40±2.93	6.61±2.27
InfoGraph [37]+SC	60.92±2.49	15.37±3.28	9.33±3.45
GraphCL [65]+KM	58.02±1.22	17.81±1.94	11.33±0.56
GraphCL [65]+SC	57.83±0.61	16.97±1.25	10.10±0.65
JOAO [66]+KM	58.34±1.46	18.73±2.62	11.06±1.79
JOAO [66]+SC	57.84±0.88	17.12±2.13	10.55±0.84
DGLC(Ours)	**61.15±1.44**	**19.98±1.41**	12.17±2.03

The best result is highlighted in bold. N/A denotes the results are unavailable (out of memory or the running time over 24 h)

Table 11. The experiment results are shown in Tables 12 and 13. We can see that almost all graph kernels show low efficiency and bad clustering performance when handling large-scale datasets, some of them are too time-consuming. While the proposed DGLC method shows superiority compared with graph kernels and graph representation learning methods. DGLC obtains the best clustering performance in most cases. Besides, the experiment on

COLLAB, which contains 3 classes, also demonstrates the effectiveness of the proposed DGLC method in processing datasets containing more than 2 classes.

5 Conclusion

This work has studied the problem of graph-level clustering and proposed an end-to-end deep graph-level clustering method based on deep graph neural networks. The proposed DGLC method leverages the powerful representation learning capability of GIN and defines an explicit clustering objective to help learn cluster-favor representations for graph-level clustering. We compared the proposed method with two types of baselines, one is based on graph kernels followed by spectral clustering and the other is based on graph-level representation learning followed by *k*-means and spectral clustering. The experiments on six graph datasets have shown that our method has much higher clustering accuracy than the baselines.

Acknowledgements This work is in part supported by the National Natural Science Foundation of China (Grants No. 62376236 and No. U21A20472), the Natural Science Foundation of Fujian Province (Grant No.2020J01130193), and Shenzhen Research Institute of Big Data (No.T00120210002).

References

1. Newman ME (2006) Modularity and community structure in networks. Proc Natl Acad Sci 103(23):8577–8582
2. Gilmer J, Schoenholz S.S, Riley P.F, Vinyals O, Dahl G.E (2017) Neural message passing for quantum chemistry. In: Proceedings of the international conference on machine learning, pp 1263–1272 . PMLR
3. LIN YSK, Bashir AK (2023) Keylight: intelligent traffic signal control method based on improved graph neural network. IEEE Transactions on Consumer Electronics, 1–1
4. Dong L, Zhang H, Yang K, Zhou D, Shi J, Ma J (2022) Crowd counting by using top-k relations: a mixed ground-truth CNN framework. IEEE Trans Consum Electron 68(3):307–316
5. Zhang R, Xie F, Sun R, Huang L, Liu X, Shi J (2022) Spatial-temporal dynamic semantic graph neural network. Neural Comput Appl 34(19):16655–16668
6. Liu L, Zhang H, Zhou D, Shi J (2023) Toward fashion intelligence in the big data era: State-of-the-art and future prospects. IEEE Trans Consumer Electron, 1–1
7. Wang Y, Cao J, Tao H (2021) Graph convolutional network with multi-similarity attribute matrices fusion for node classification. Neural Comput Appl, 1–11
8. Zhang B, Guo X, Tu Z, Zhang J (2022) Graph alternate learning for robust graph neural networks in node classification. Neural Comput Appl 34(11):8723–8735
9. Ju W, Qin Y, Yi S, Mao Z, Zheng K, Liu L, Luo X, Zhang M (2023) Zero-shot node classification with graph contrastive embedding network. Trans Mach Learn Res
10. Wu Z, Zhang Z, Fan J (2023) Graph convolutional kernel machine versus graph convolutional networks. Adv Neural Inform Process Syst
11. Fan J, Tian Z, Zhao M, Chow TWS (2018) Accelerated low-rank representation for subspace clustering and semi-supervised classification on large-scale data. Neural Netw 100:39–48
12. Lin Z, Kang Z, Zhang L, Tian L (2021) Multi-view attributed graph clustering. IEEE Trans Knowledge Data Eng
13. Fan J (2021) Large-scale subspace clustering via k-factorization. In: Proceedings of the ACM SIGKDD conference on knowledge discovery & data mining. KDD '21, pp 342–352. Association for Computing Machinery, New York, NY, USA
14. Cai J, Fan J, Guo W, Wang S, Zhang Y, Zhang Z (2022) Efficient deep embedded subspace clustering. In: Proceedings of the IEEE/CVF conference on computer vision and pattern recognition (CVPR), pp 1–10
15. Fan J, Tu Y, Zhang Z, Zhao M, Zhang H (2022) A simple approach to automated spectral clustering. Adv Neural Inform Process Syst 35:9907–21
16. Gao X, Ma X, Zhang W, Huang J, Li H, Li Y, Cui J (2022) Multi-view clustering with self-representation and structural constraint. IEEE Trans Big Data 8(4):882–893
17. Cai J, Wang S, Xu C, Guo W (2022) Unsupervised deep clustering via contractive feature representation and focal loss. Pattern Recogn 123:108386
18. Yan S, Xu D, Zhang B, Zhang H-J, Yang Q, Lin S (2006) Graph embedding and extensions: a general framework for dimensionality reduction. IEEE Trans Pattern Anal Mach Intell 29(1):40–51
19. Cai H, Zheng VW, Chang KC-C (2018) A comprehensive survey of graph embedding: problems, techniques, and applications. IEEE Trans Knowl Data Eng 30(9):1616–1637
20. Li T, Zhang Y, Liu H, Xue G, Liu L (2022) Fast compressive spectral clustering for large-scale sparse graph. IEEE Trans Big Data 8(1):193–202
21. Subramanya A, Bilmes JA (2009) Entropic graph regularization in non-parametric semi-supervised classification. Adv Neural Inform Process Syst, 22
22. Bhagat S, Cormode G, Muthukrishnan S (2011) Node classification in social networks. In: Social network data analytics, pp 115–148. Springer, ???
23. Kipf TN, Welling M (2017) Semi-supervised classification with graph convolutional networks. Proceedings of the international conference on learning representations
24. Xu K, Hu W, Leskovec J, Jegelka S (2019) How powerful are graph neural networks? In: Proceedings of the international conference on learning representations
25. Chen Z, Fu L, Xiao S, Wang S, Plant C, Guo W (2023) Multi-view graph convolutional networks with differentiable node selection. ACM Trans Knowl Discov Data 18(1):1–21
26. Wang C, Pan S, Hu R, Long G, Jiang J, Zhang C (2019) Attributed graph clustering: a deep attentional embedding approach. In: Proceedings of the 28th international joint conference on artificial intelligence, pp 3670–3676
27. Bo D, Wang X, Shi C, Zhu M, Lu E, Cui P (2020) Structural deep clustering network. In: Proceedings of the web conference, pp 1400–1410
28. Zhu H, Koniusz P (2021) Simple spectral graph convolution. In: Proceedings of the international conference on learning representations
29. Guo L, Dai Q (2022) End-to-end variational graph clustering with local structural preservation. Neural Comput Appl, 1–16
30. Vishwanathan SVN, Schraudolph NN, Kondor R, Borgwardt KM (2010) Graph kernels. J Mach Learn Res 11:1201–1242

31. Yanardag P, Vishwanathan S (2015) Deep graph kernels. In: Proceedings of the 21th ACM SIGKDD international conference on knowledge discovery & data mining, pp 1365–1374
32. Wu Z, Pan S, Chen F, Long G, Zhang C, Philip SY (2020) A comprehensive survey on graph neural networks. IEEE Trans Neural Netw Learn Syst 32(1):4–24
33. Rong Y, Xu T, Huang J, Huang W, Cheng H, Ma Y, Wang Y, Derr T, Wu L, Ma T (2020) Deep graph learning: foundations, advances and applications. In: Proceedings of the 26th ACM SIGKDD international conference on knowledge discovery & data mining, pp 3555–3556
34. Sun Z, Ding C, Fan J (2023) Lovász principle for unsupervised graph representation learning. Adv Neural Inform Process Syst
35. Chen Z, Fu L, Yao J, Guo W, Plant C, Wang S (2023) Learnable graph convolutional network and feature fusion for multi-view learning. Inform Fusion 95:109–119
36. Zhang M, Cui Z, Neumann M, Chen Y (2018) An end-to-end deep learning architecture for graph classification. In: Proceedings of the AAAI conference on artificial intelligence, vol 32
37. Sun FY, Hoffman J, Verma V, Tang J (2020) Infograph: unsupervised and semi-supervised graph-level representation learning via mutual information maximization. In: Proceedings of the international conference on learning representations
38. Doshi S, Chepuri SP (2022) Graph neural networks with parallel neighborhood aggregations for graph classification. IEEE Transactions on signal processing, 1–14
39. Cai J, Zhang Y, Fan J (2023) Self-discriminative modeling for anomalous graph detection. arXiv preprint arXiv:2310.06261
40. Ju W, Gu Y, Chen B, Sun G, Qin Y, Liu X, Luo X, Zhang M (2023) Glcc: a general framework for graph-level clustering. In: Proceedings of the AAAI conference on artificial intelligence, vol 37, pp 4391–4399
41. Ng A, Jordan M, Weiss Y (2001) On spectral clustering: Analysis and an algorithm. Adv Neural Inform Process Syst, 14
42. Fan J, Chow TW (2017) Sparse subspace clustering for data with missing entries and high-rank matrix completion. Neural Netw 93:36–44
43. Xu K, Tang K, Su Z (2023) Deep multi-view subspace clustering via structure-preserved multi-scale features fusion. Neural Comput Appl 35(4):3203–3219
44. Qiao D, Ding C, Fan J (2023) Federated spectral clustering via secure similarity reconstruction. Adv Neural Inform Process Syst
45. Kondor R, Pan H (2016) The multiscale laplacian graph kernel. Adv Neural Inform Process Syst, 29
46. Du SS, Hou K, Salakhutdinov RR, Poczos B, Wang R, Xu K (2019) Graph neural tangent kernel: Fusing graph neural networks with graph kernels. Adv Neural Inform Process Syst, 32
47. Togninalli M, Ghisu E, Llinares-López F, Rieck B, Borgwardt K (2019) Wasserstein weisfeiler-lehman graph kernels. Adv Neural Inform Process Syst, 32
48. Gärtner T, Flach P, Wrobel S (2003) In: Learning theory and kernel machines: 16th annual conference on learning theory and 7th kernel workshop, pp 129–143 . Springer
49. Shervashidze N, Schweitzer P, Van Leeuwen EJ, Mehlhorn K, Borgwardt KM (2011) Weisfeiler-lehman graph kernels. J Mach Learn Res, 12(9).
50. Liu Y, Tu W, Zhou S, Liu X, Song L, Yang X, Zhu E (2022) Deep graph clustering via dual correlation reduction. In: Proceedings of the AAAI conference on artificial intelligence
51. Cai J, Guo W, Fan J (2022) Unsupervised deep discriminant analysis based clustering. arXiv preprint arXiv:2206.04686
52. Ju W, Yang J, Qu M, Song W, Shen J, Zhang M (2022) Kgnn: Harnessing kernel-based networks for semi-supervised graph classification. In: Proceedings of the Fifteenth ACM international conference on web search and data mining, pp 421–429
53. Ju W, Luo X, Ma Z, Yang J, Deng M, Zhang M (2022) Ghnn: graph harmonic neural networks for semi-supervised graph-level classification. Neural Netw 151:70–79
54. Hartigan JA, Wong MA (1979) Algorithm as 136: A k-means clustering algorithm. J R Stat Soc Series C Appl Stat 28(1):100–108
55. Grover A, Leskovec J (2016) node2vec: Scalable feature learning for networks. In: Proceedings of the 22nd ACM SIGKDD international conference on knowledge discovery & data mining, pp 855–864
56. Narayanan A, Chandramohan M, Venkatesan R, Chen L, Liu Y, Jaiswal S (2017) graph2vec: Learning distributed representations of graphs. arXiv preprint arXiv:1707.05005
57. Shervashidze N, Vishwanathan S, Petri T, Mehlhorn K, Borgwardt K (2009) Efficient graphlet kernels for large graph comparison. In: Proceedings of the artificial intelligence and statistics, pp 488–495. PMLR
58. Borgwardt KM, Kriegel HP (2005) Shortest-path kernels on graphs. In: Proceedings of the IEEE international conference on data mining, p 8 . IEEE
59. Kriege N, Mutzel P (2012) Subgraph matching kernels for attributed graphs. arXiv preprint arXiv:1206.6483
60. Nikolentzos G, Meladianos P, Vazirgiannis M (2017) Matching node embeddings for graph similarity. In: Proceedings of the Thirty-first AAAI conference on artificial intelligence
61. Zhou J, Cui G, Hu S, Zhang Z, Yang C, Liu Z, Wang L, Li C, Sun M (2020) Graph neural networks: a review of methods and applications. AI Open 1:57–81
62. Zhang C, Song D, Huang C, Swami A, Chawla NV (2019) Heterogeneous graph neural network. In: Proceedings of the 25th ACM SIGKDD international conference on knowledge discovery & data mining, pp 793–803
63. Ju W, Gu Y, Luo X, Wang Y, Yuan H, Zhong H, Zhang M (2023) Unsupervised graph-level representation learning with hierarchical contrasts. Neural Netw 158:359–368
64. Veličković P, Fedus W, Hamilton WL, Liò P, Bengio Y, Hjelm RD (2019) Deep graph infomax. In: Proceedings of the international conference on learning representations
65. You Y, Chen T, Sui Y, Chen T, Wang Z, Shen Y (2020) Graph contrastive learning with augmentations. Adv Neural Inf Process Syst 33:5812–5823
66. You Y, Chen T, Shen Y, Wang Z (2021) Graph contrastive learning automated. In: Proceedings of the international conference on machine learning, pp 12121–12132 . PMLR
67. Chen T, Kornblith S, Norouzi M, Hinton G (2020) A simple framework for contrastive learning of visual representations. In: Proceedings of the international conference on machine learning, pp 1597–1607 . PMLR
68. Hjelm R.D, Fedorov A, Lavoie-Marchildon S, Grewal K, Bachman P, Trischler A, Bengio Y (2019) Learning deep representations by mutual information estimation and maximization. In: Proceedings of the international conference on learning representations
69. Nowozin S, Cseke B, Tomioka R (2016) f-gan: Training generative neural samplers using variational divergence minimization. Adv Neural Inform Process Syst, 29
70. Maaten L, Hinton G (2008) Visualizing data using t-sne. J Mach Learn Res 9(11):2579–2605
71. xXie J, Girshick R, Farhadi A (2016) Unsupervised deep embedding for clustering analysis. In: Proceedings of the international conference on machine learning, pp 478–487 . PMLR

72. Kriege NM, Giscard PL, Wilson R (2016) On valid optimal assignment kernels and applications to graph classification. Adv Neural Inform Process Syst, 29
73. Johansson F, Jethava V, Dubhashi D, Bhattacharyya C (2014) Global graph kernels using geometric embeddings. In: Proceedings of the international conference on machine learning, pp 694–702 . PMLR
74. Xu H, Liu J, Luo D, Carin L (2022) Representing graphs via Gromov–Wasserstein factorization. IEEE Trans Pattern Anal Mach Intell 45(1):999–1016
75. Fey M, Lenssen JE (2019) Fast graph representation learning with pytorch geometric. arXiv preprint arXiv:1903.02428
76. Siglidis G, Nikolentzos G, Limnios S, Giatsidis C, Skianis K, Vazirgiannis M (2020) Grakel: a graph kernel library in python. J Mach Learn Res 21(54):1–5